Thin Film of Cobalt Hexacyanocobaltate

MS Thesis

Submitted to

Indian Institute of Science Education and Research Pune towards the partial fulfilment of BS-MS Dual degree

By

Jainendra Singh

20141011

Supervisor: **Dr. Nirmalya Ballav**

Department of Chemistry

IISER Pune

October 2019

Certificate

This is to certify that this dissertation entitled "**Thin Film of Cobalt Hexacyanocobaltate**" towards the partial fulfilment of the BS-MS dual degree programme at the Indian Institute of Science Education and Research, Pune represents study/work carried out by **Jainendra Singh** under the supervision of **Dr. NirmalyaBallav, Department of Chemistry, Indian Institute of Science Education and Research,** Pune during the academic year 2019.

Dr. NirmalyaBallav

(Supervisor)

Associate Professor

Department of Chemistry, IISER Pune

20/10/2019

निर्मल्या बल्लव / Nirmalya Ballav
सहयोगी प्राध्यापक, रसायनशास्त्र / Associate Professor, Chemistry
भारतीय विज्ञान शिक्षा एवं अनुसंधान संस्थान
Indian Institute of Science Education & Research
पुणे / Pune - 411 008, India

Jainendra Singh

20141011

IISER Pune

Declaration

I hereby declare that the matter embodied in the report entitled "**Thin Film of Cobalt Hexacyanocobaltate**" are the results of the work carried out by me at the Department of Chemistry, IISER Pune, under the supervision of Dr. NirmalyaBallav and the same has not been submitted elsewhere for any other degree.

Dr. NirmalyaBallav

(Supervisor)

Associate Professor

Department of Chemistry, IISER Pune

20/10/2019

निर्मल्या बल्लव / Nirmalya Ballav
सहयोगी प्राध्यापक, रसायनशास्त्र / Associate Professor, Chemistry
भारतीय विज्ञान शिक्षा एवं अनुसंधान संस्थान
Indian Institute of Science Education & Research
पुणे / Pune - 411 008, India

Jainendra Singh

20141011

IISER Pune

Dedicated to

My Mother and Father

Acknowledgement

First of all, I would like to thank my supervisor Dr. Nirmalya Ballav for giving me an opportunity to work in his lab. Without his guidance and encouragements it would not have been possible. His advices regarding academic and non-academic problems has helped me. I am thankful for his faith and trust in me in various ups and downs.

A sincere gratitude to Prof. T.A. Jung and Dr. J. Dreiser of PSI, Switzerland for XAS/XMCD measurements.

The big credit for my science and research learnings goes to Dr. Shammi Rana and also to his motivations which helped me work hard. I would like to thank Dr. Plawan Kumar Jha, Dr. Sujit Bhand, Kriti Gupta for helping me on the problems during my project. I would like to thank Debashree, Ashwini, Pooja, Aswani, Gopi, Ishan, Pranay and former lab mates for providing friendly decorum in the lab.

I am indebted to my close friends Prakash, Vaibhav, Daman, Anurag, Sagar for sharing the funny moments.

Last but not the least, an utmost acknowledgement to my family, Mother, Father, Rocky, Iti, Jaswant for all the love and emotional support.

Contents

List of Schemes and Figures

1. Abstract

Prussian blue analogues (PBAs) have recently acquired a great deal of attention because of their promise in the fields of energy storage, drug delivery, thermochromic materials, magnetic materials and many more. Herein, for the first time we have fabricated high-quality thin film of cobalt hexacyanocobaltate (CoHCC) on both Au and Si substrates. This was achieved by a low cost solution-processable method involving layer-by-layer (LbL) approach. The thin film was found to be insulating in nature with the resistance of ~10^9 Ω. Doping by HCl vapors resulted in improved electrical conductivity of the thin film. Both the Au and Si substrates were functionalized by organic monolayers of thiol and alkene prior to the thin film deposition. FESEM and HRTEM analyses of isolated material from the thin film consistently revealed cube-like morphology. Significant difference in K^+ alkali ion concentration between the thin film and bulk was detected by EDXS technique. Interestingly, appreciable difference in the intrinsic magnetic moments of thin film and bulk CoHCC was evinced by XAS and XMCD techniques.

2. Introduction

2.1 Prussian Blue Analogues

The general formula for PBAs is represented as $A_xM_y[M'(CN)_6]_z.xH_2O$ where A corresponds to alkali metal ions eg. Na^+, K^+ and M and M' indicates transition metal ions. PBAs have open framework structure with nanoporous wide channels allowing rapid ionic conduction for high rate capability. They have high specific capacity for alkali metals and alkali earth metals which has been proven to play a vital role in thermal and photoinduced electron transfer.[1] The uptake of enough K^+ ions in the interstitial sites of FeCo PBA was reported to undergo magnetization state change from a paramagnet to ferrimagnet state.[2]

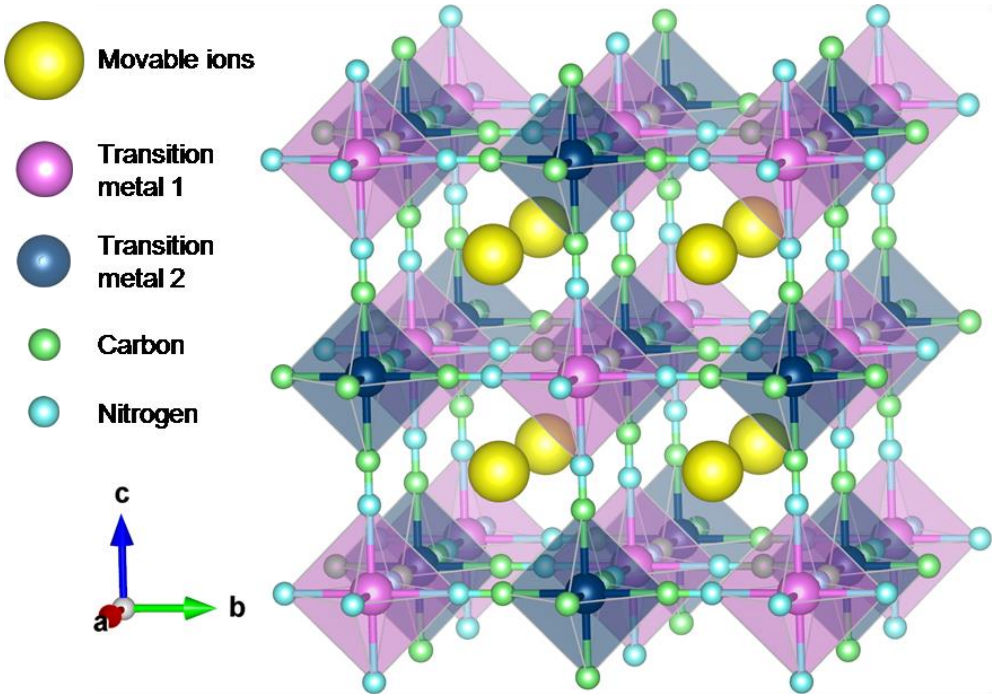

Figure 1: *Schematic showing crystal structure of PBAs (adopted from Ref.* [3]*)*

PBAs crystallizes in the face centered cubic structure forming coordination cubes involving M-CN-M' links. It could lead to diverse range of applications like magnetic, electronic, catalytic etc. by easily changing M, M' metal ions or the same metal with different oxidation states.[4]. For electronic applications transition metals with large number of unbonded electrons like Fe, Cu, Co have been the good competitors. For

magnetic application, transition metals with large number of unpaired electrons like Cr, Mn performed excellently.[4] The cyanide bridge in PBAs between transition metals is special and could encourage strong magnetic coupling between paramagnetic centres. PBAs are commonly synthesized by solution precipitation method. These factors allow substantial control and tunability in PBAs for the diverse applications.

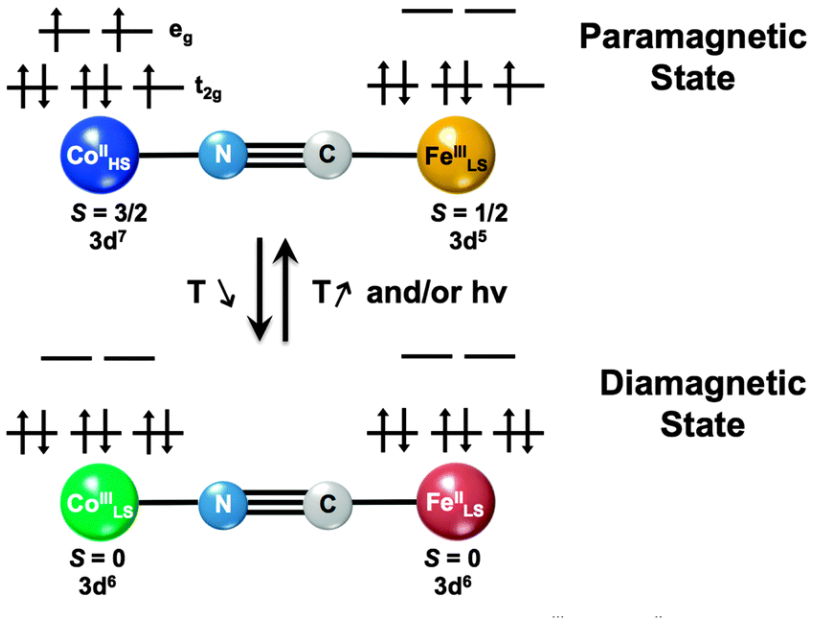

Figure 2: *Schematic demonstrating photoinduced charge transfer (adopted from Ref.* [5]*)*

PBAs could undergo phase transitions stimulated by pressure, temperature, or light irradiation.[6] Thermal or photo induced charge transfer induced spin transition has been widely studied in FeCo PBAs. PBA of FeCo containing cesium as the alkali metal ion, exhibited thermally induced electron transfer from Co(ll) to Fe(lll) at low temperature.[7] This transfer was affected by the movement of Cesium ions back to the center of interstitial sites at low temperatures. In another PBA of FeCo, parallel alignment of Fe and Co ions in the photoexcited state was investigated by XAS and XMCD.[8]. A PBA of vanadium hexacyanochromate exhibited spontaneous magnetic ordering at T_c = 315 K suggesting transition metal hexacyanocomplexes as the promising candidate for the construction of high T_c magnets.[9]

2.2 Salient features of Cobalt Hexacyanocobaltate (CoHCC)

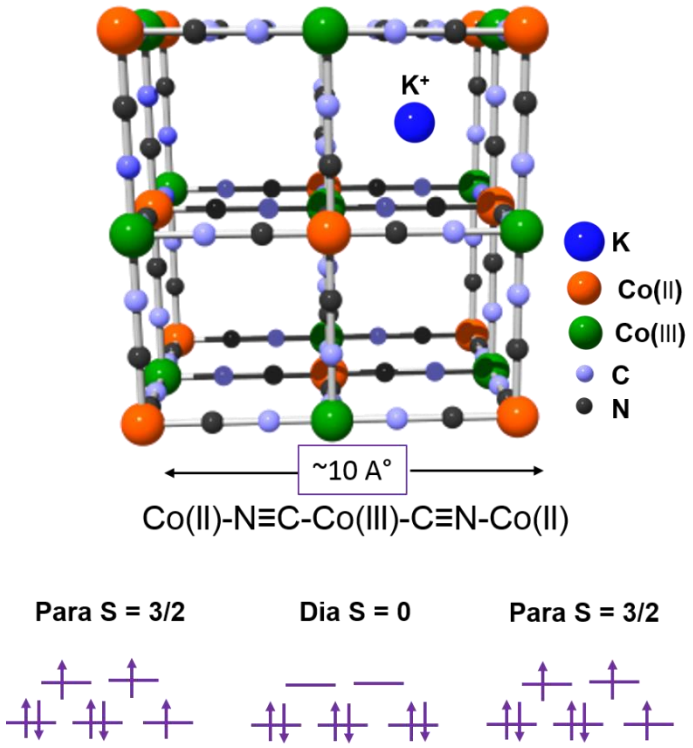

Figure 3: *Schematic unveiling structure of CoHCC and spin states of Co (cubic structure imported from Ref.* [10] *with modifications)*

CoHCC in the bulk form is a thermochromic material which is reported to change color from pink to blue as the temperature is increased.[9] CoHCC has been utilized as an anode material for nonaqueous potassium ion batteries delivering highly reversible capacity of 324.5 $mAhg^{-1}$ at a current density of 0.1 Ag^{-1}.[11] Due to its porous framework, CoHCC has been proven to have high affinity towards sorption and desorption towards ammonia.[12] CoHCC modified bismuth vanadate was utilized for photoelectrochemical water oxidation.[13]

Synthesis of PBAs in the bulk form have been known for a long time but bringing the PBAs in the thin film configuration by a solution deposition method using LbL approach is still a challenging task. Lbl offers certain novel features for example (1) highly crystalline and oriented growth, (2) control over thickness, (3) limiting the interpenetration of coordination polymers. Many studies have shown that properties of the material in the thin film configuration might differ from the bulk.[12] Earlier work from our group on

spontaneous reduction of Cu(ll) to Cu(l) in copper hexacyanoferrate thin film was evinced at solid-liquid interface without the use of any external reducing agent.[10]

Motivated by the salient features of CoHCC in the bulk form and lack of CoHCC thin film in the literature, we decided to fabricate CoHCC thin film and explore its properties. Herein, we report the first time fabrication of a high-quality CoHCC thin film on both the gold and silicon substrates by LbL approach. Self-assembled monolayer (SAM) of 11-mercaptoundecanoic acid (MUDA) was prepared on Au substrate, an organic monolayer of Undecylenic acid (UDA) was grafted on Si substrate prior to the thin film deposition.

3. Materials and Methods

3.1 Chemicals Required

Cobalt (ll)acetate tetrahydrate ($Co(OAc)_2.4H_2O$), Potassium hexacyanocobaltate (lll) ($K_3[Co(CN)_6]$), Hydrogen fluoride (HF) (40%), Undecylenic acid (UDA)

3.2 Substrates Required

Gold coated silicon wafer, P-type Silicon wafer

3.3 Substrates Cleaning

For cleaning, Au and Si substrates were sonicated in a series of solvents starting with distilled water, acetone, methanol, isopropanol and then treated with piranha solution (H2SO4:H2O2 = 3:1)

4. Synthesis and Fabrication

Functionalization of Au Substrate: Mercaptouncanoic acid (MUDA) is used as a Self-assembled monolayer (SAM) on Au substrate. Cleaned Au substrate was dipped in 1mM MUDA solution (ethanol : acetic acid = 9:1) to obtain carboxyl-terminated functionalized Au substrate. Here, tail end of mercaptoundecanoic acid (i.e. SH) interacts with Au by HSAB principle forming the Au-S semicovalent bond.

Functionalization of Si Substrate: The functionalization procedure on Si is different from Au and has been followed from the reported article with slight modifications.[14]. Cleaned Si substrate was oxidized with piranha solution for 45 min and then immersed in 40% HF solution for 2 min to remove the oxide layer from silicon surface. HF treated

silicon substrate was then anodized in the HF/ethanol = 1:1 (HF = 40% and ethanol = 100%) mixture at an applied current of 80 mA/cm^2 for 30 seconds. This hydrogen terminated porous silicon was then kept in neat undecylenic acid (UDA) solution at 150 °C for 24 hours as shown in Fig. 4. In this step, hydrosilylation reaction occurs between UDA and hydrogen-terminated silicon which proceeds via thermally driven radical pathway.[15] This leads to the formation of Si-C high strength bond and thereby functionalization of Si substrate with carboxyl-termination.

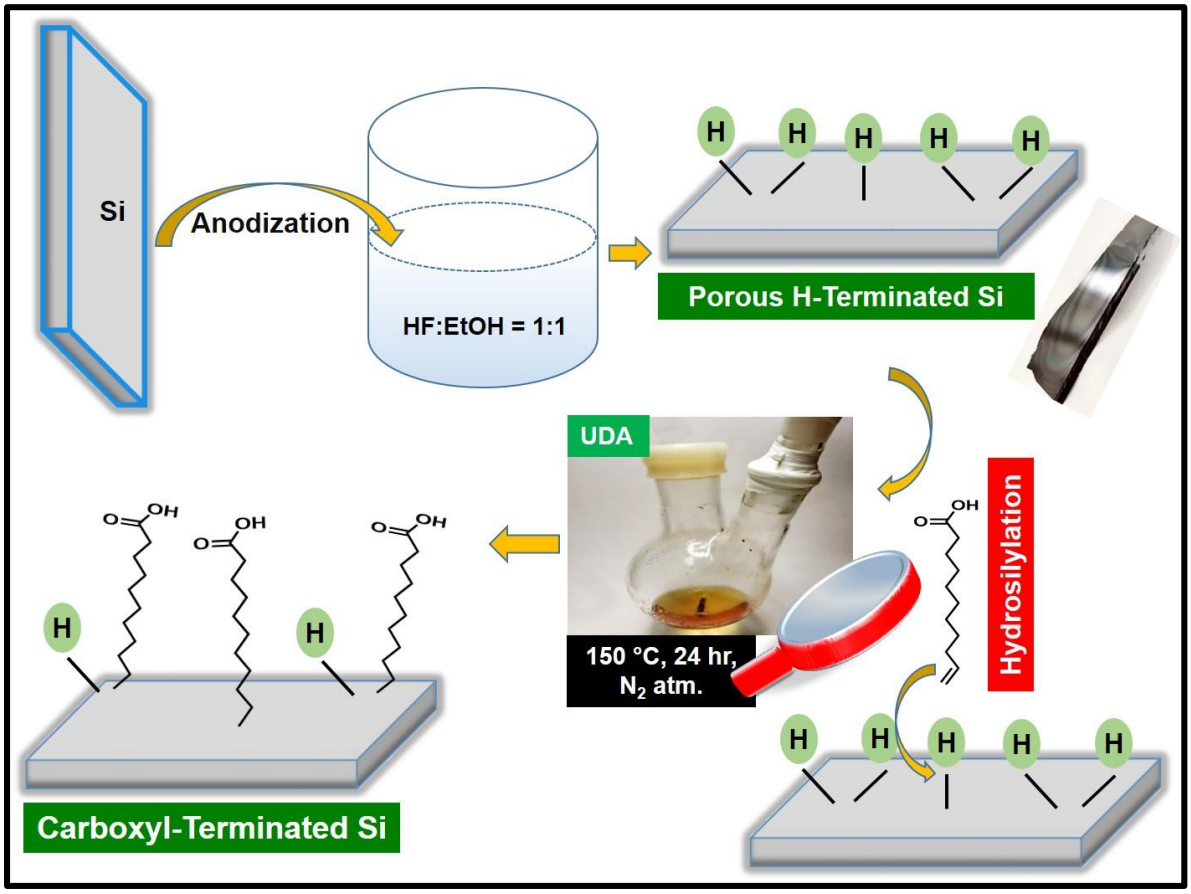

Figure 4: *Schematic evincing procedure for functionalizing Si substrate. Hydrosilylation reaction driven by radical pathway*.

Fabrication of CoHCC Thin Film: The thin film was fabricated by solution deposition method involving LbL approach. The functionalized Au and Si substrates were first dipped in 2 mM ethanolic solution of cobalt acetate ($Co(OAc)_2$) kept at 60 °C for 30 min accompanied by washing with methanol and drying as shown in Fig. 7a. Substrates were then dipped in aqueous ethanolic (H_2O:C_2H_5OH = 3:7) potassium hexacyanocobaltate ($K_3[Co(CN)_6]$) solution kept at 60 °C for 30 min accompanied by

washing with methanol and drying. This completes one cycle of LbL growth method and the same procedure was repeated upto 20 cycles.

Synthesis of Bulk CoHCC: Bulk CoHCC was synthesized by simple aqueous solution precipitation method. In this, 0.1 M aqueous $Co(OAc)_2$ solution was mixed with 0.05 M aqueous $K_3Co(CN)_6$ solution under continuous stirring for 3 hours and then left undisturbed for 24 hours as shown in Fig. 5. The obtained precipitate was then centrifuged and washed 3 times with DI water. The washed precipitate was then vacuum dried for 3 hours at 110 °C.

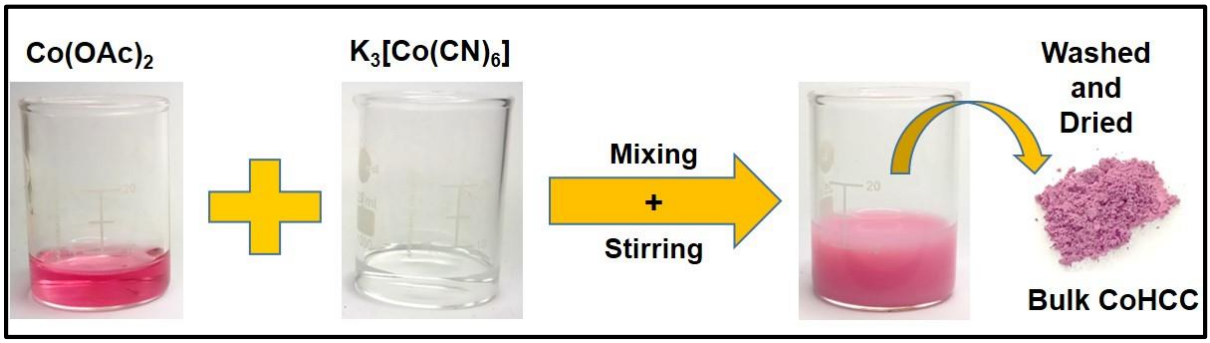

Figure 5: *Illustration demonstrating procedure for synthesizing bulk CoHCC.*

HCl Doping: To modulate the electronic conductivity in both CoHCC bulk and thin film were exposed to HCl vapours. CoHCC bulk and thin film were first activated at 110 °C to remove the water molecules and then HCl vapours were allowed to pass in activated CoHCC bulk and thin film under vacuum at room temperature for 20 hours as shown in Fig. 6.

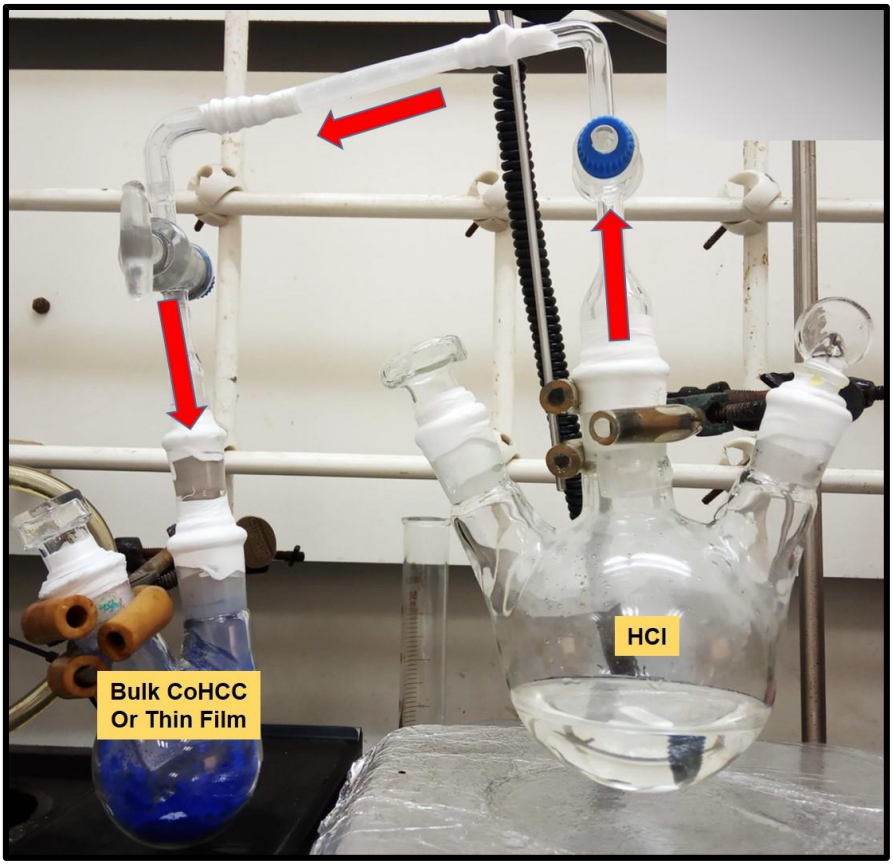

Figure 6: *Representation displaying HCl doping procedure in CoHCC bulk.*

5. Results and Discussion

The bulk form of CoHCC has been reported as $Co_3[Co(CN)_6]_2.nH_2O$ where Co(lll) is linked with C and Co(ll) is linked with N of nitrile group experiencing strong ligand field and weak ligand field respectively and thereby forming Co(lll)-C≡N-Co(ll) link. Here, Co(lll) is in the low spin state with S = 0 and acts as a diamagnetic center while Co(ll) is in the high spin state with S = 3/2 acting as a paramagnetic center.

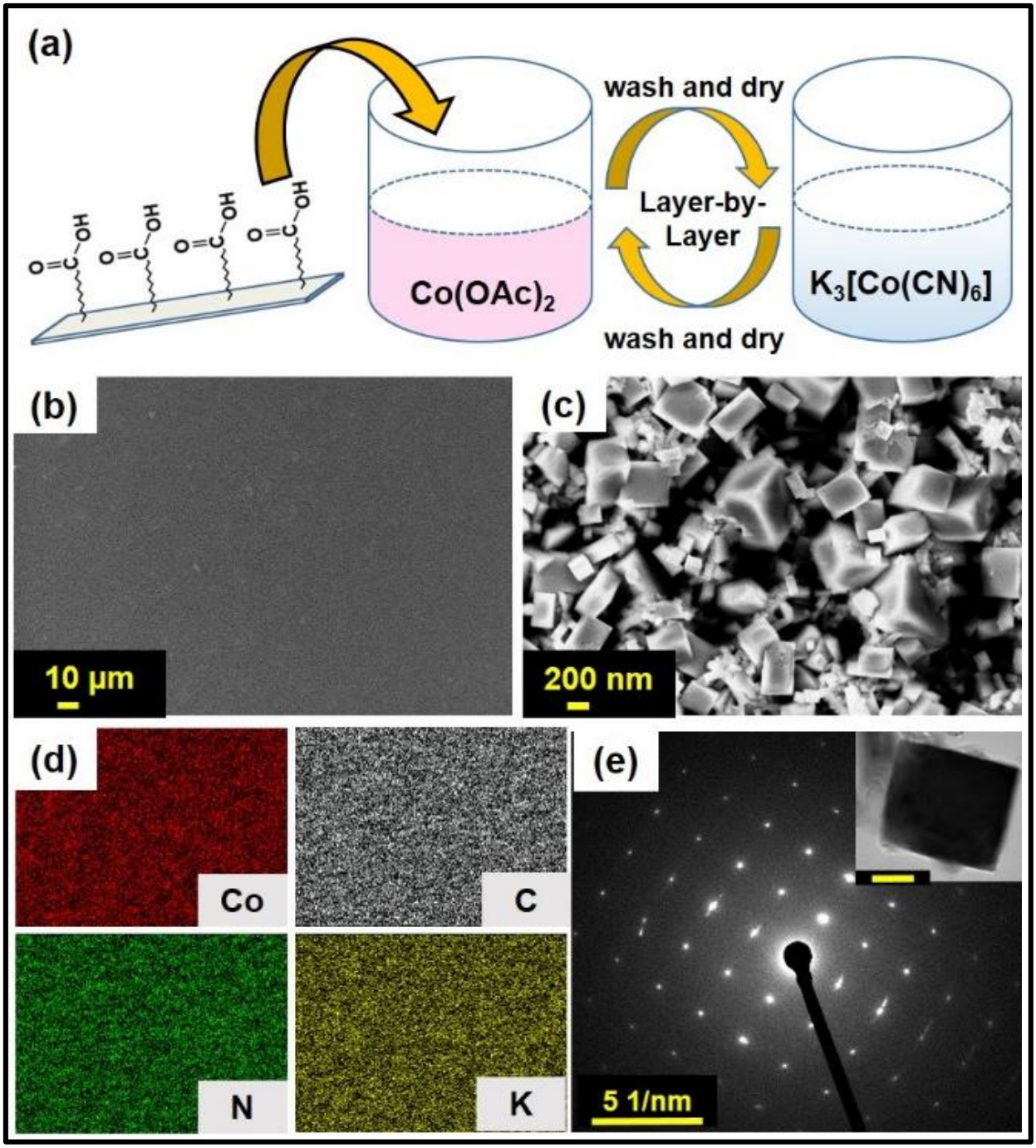

Figure 7: *(a) Schematic demonstrating layer-by-layer growth method, (b) and (c) Zoomed-out and zoomed-in CoHCC thin film FESEM images respectively, (d) EDXS mapping of the CoHCC thin film across the plane, (e) SAED pattern acquired by HRTEM of the material extracted from the thin film, inset displays the cube observed in the extracted material from the thin film*

The fabricated thin film was characterized by various techniques. Field emission scanning electron microscope (FESEM) revealed uniform, smooth and high-quality thin film having cube-like morphology on both Au and Si substrates as shown in Fig. 7(b,c). The thickness of the thin film on Si substrate was measured by using cross-sectional FESEM and was observed to be ~550 nm as shown in Fig. 8.

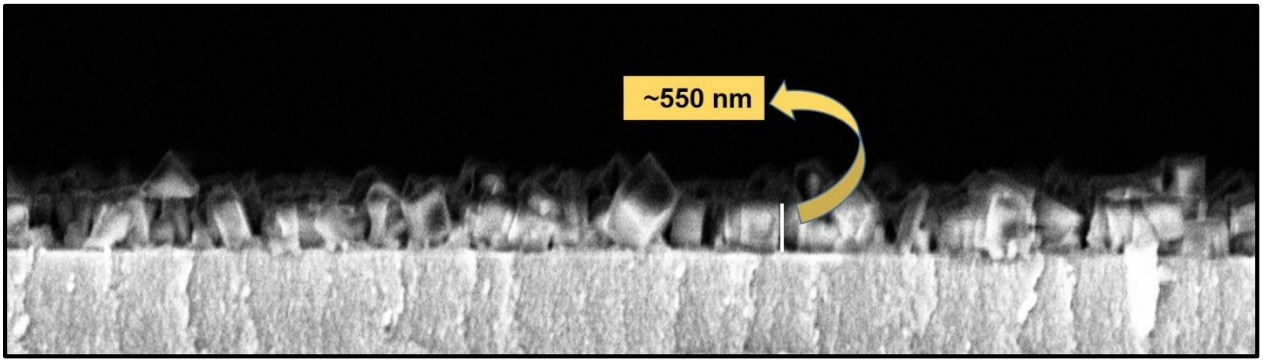

Figure 8: *Cross-sectional FESEM image of CoHCC thin film on Si substrate.*

While the thickness on Au substrate was found to be ~200 nm. The reason behind the discrepancy in the thickness of the thin film on Au and Si substrates might be attributed to different functionalization procedure. Homogeneous distribution of all the elements (Co, C, N, K) across the thin film was observed through the elemental mapping by energy dispersive X-ray spectroscopy (EDXS) technique (Fig 7d).

Elements	C	N	O	K	Co
Bulk CoHCC Atomic %	38.96	51.73	3.66	**0.08**	5.56
Thin Film Atomic %	33.05	38.05	25.18	**0.85**	2.85

Figure 9: *Table showing EDXS of both the bulk and thin film CoHCC.*

Surprisingly, the thin film exhibited the presence of potassium ions which were nearly absent in the bulk form configuration (Fig. 8). This difference in the composition of alkali metal ion between thin film and the bulk form is high and significant enough to cause the properties differences. The morphology and crystallinity of the thin film was further analyzed using high-resolution transmission electron microscopy (HRTEM) and selected area electron diffraction (SAED) technique (Fig. 7e). HRTEM image of the material

extracted from the thin film exhibited cube like morphology (inset Fig. 7e). SAED pattern of the thin film revealed highly crystalline cubic nature of the thin film while the weak diffraction rings in the SAED pattern of the bulk form indicated its polycrystalline nature. Further the spacing between lattice fringes d_{TEM}=0.53 nm value was also calculated through HRTEM.

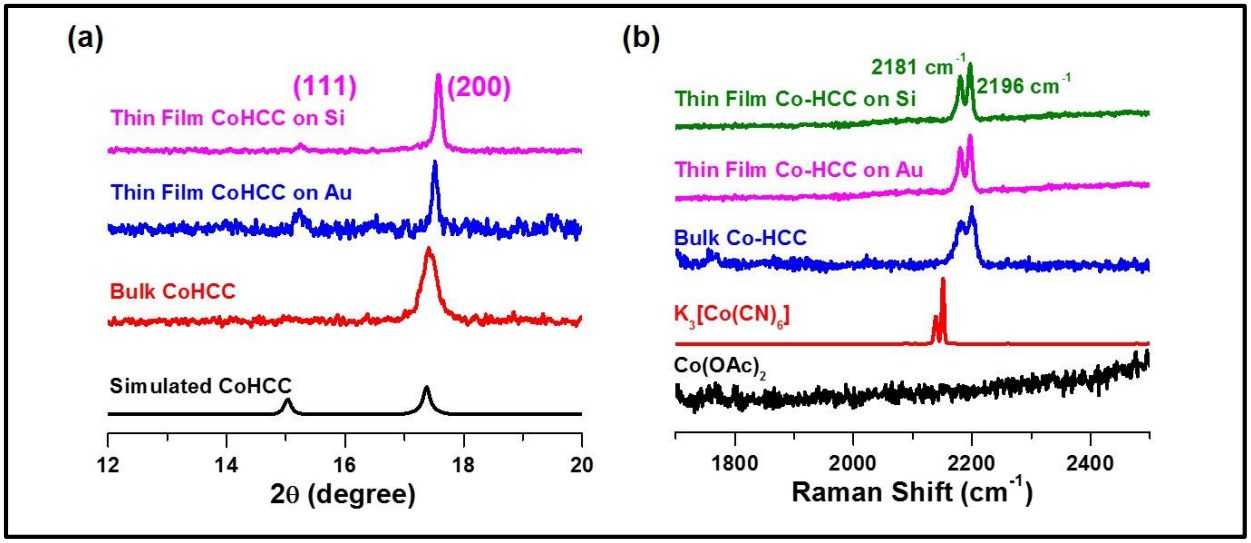

Figure 10: *(a) Out-of-plane XRD patterns of CoHCC bulk and thin film on Si and Au substrates. (b) Raman spectra of precursors $Co(OAc)_2$ and $K_3[Co(CN)_6]$, bulk CoHCC, thin film CoHCC on Au and Si substrates.*

Further crystallinity and structural study was carried out using out-of-plane X-ray diffraction technique (XRD) as shown in Fig. 10a. The two diffraction peaks at 2θ ~15.1° and ~17.5° corresponding to (111) and (200) crystallographic planes respectively were characteristic of the CoHCC in the face-centered cubic phase and matches well with the simulated XRD. Analysis of the diffraction peak at 2θ = 17.5° gives the lattice spacing value d_{XRD}=0.51 nm. This d_{XRD} value matches well with the d_{TEM} value, thereby confirming the cubic structure. To check the bonding and valence states in the CoHCC coordination network, Raman study was carried out (Fig. 10b) on both the CoHCC bulk and the thin film. The two Raman peaks at ~2181 cm^{-1} and ~2196 cm^{-1} may be attributed to the cyanide stretching frequencies arising due to the presence of mixed valence states Co(II)-C≡N-Co(III) and Co(III)-C≡N-Co(II) respectively, as predicted in an earlier report with similar PBA Copper hexacyanocobaltate (CuHCC).[16] Here the reason could be, as the

positive charge on the central atom (i.e. cobalt attached with the carbon of nitrile group) increases the bond between metal and carbon becomes shorter, thereby increasing the Raman frequency. However, the peaks in precursor $K_3[Co(CN)_6]$ at ~2138 cm^{-1} and ~2150 cm^{-1} are a significance of E_g and A_{1g} modes respectively, emerging from Co(lll)-CN free cyanide stretching.[17]

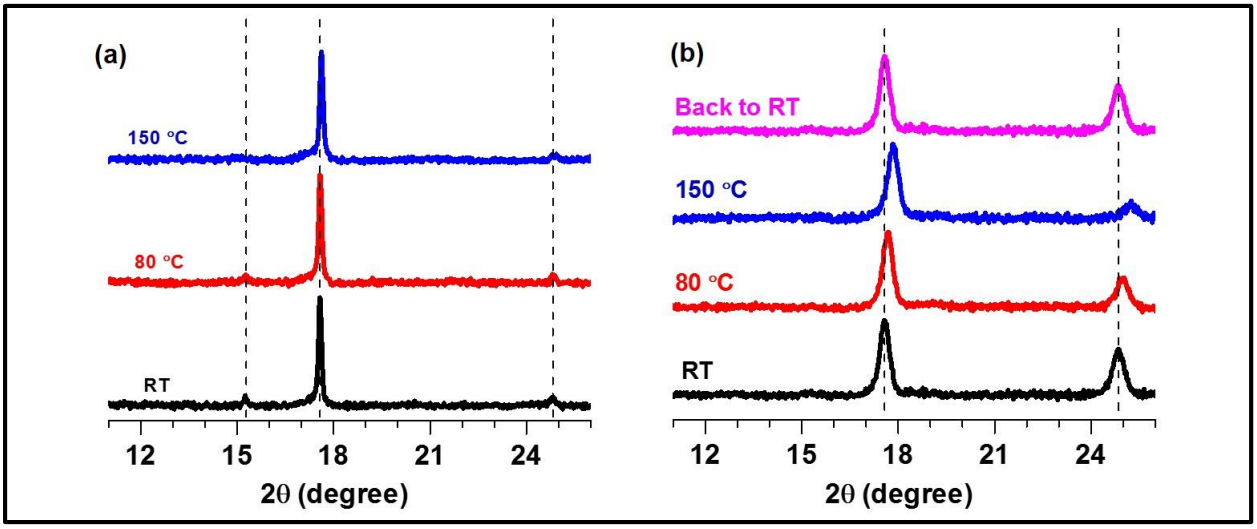

Figure 11: *Temperature dependent XRD plots of (a) CoHCC thin film, (b) CoHCC bulk.*

The thermal stability of CoHCC bulk and thin film structure was checked by variable temperature XRD (VT- PXRD) technique as shown in Fig. 11. A peak at ~15.1° corresponding to (111) plane in the thin film becomes absent at 150 °C. The XRD peaks in bulk CoHCC experienced blue shift as the temperature is increased from room-temperature to 150 °C (Fig. 11b). According to the Bragg's law $2dSin\theta=n\lambda$, increase in 2θ implies decrease in d value of the crystal structure. This change may be attributed to shrinking of the crystal structure due to loss of water molecules from the bulk CoHCC. But, interestingly this shift was not observed in the CoHCC thin film as the temperature is increased. Overall the crystallinity of both the CoHCC bulk and thin film was retained upto 150 °C.

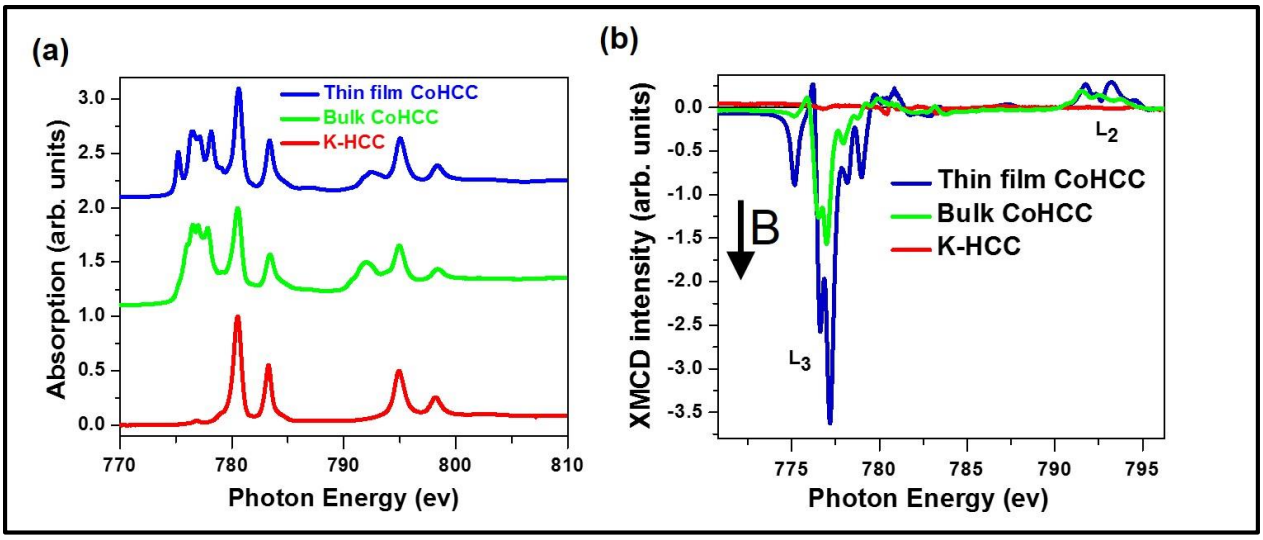

Figure 12: *(a) XAS spectra at L-edge of K-HCC, bulk CoHCC and thin film CoHCC. (b) XMCD spectra at L-edge of K-HCC, bulk CoHCC and thin film CoHCC. 6*

To understand the valence and spin states, X-ray absorption spectroscopy (XAS) is one of the powerful experimental technique.[18] Low temperature XAS studies at 2K were performed at the $L_{2,3}$ -edge for cobalt ions in both the CoHCC bulk and thin film (Fig. 12). The peaks at 780.5 eV and 783.5 eV in potassium hexacyanocobaltate ($K_3[Co(CN)_6]$) are a signature of cobalt in Co(lll) configuration as expected. XAS spectra of both CoHCC bulk and thin film exhibits the peaks at 776.5 eV, 777.0 eV and 777.8 eV which are arising from Co(ll) state while the peaks at 780.5 eV and 783.2 eV are an indication of Co(lll) state.[8] Interestingly, a distinctive peak at 775.2 eV arising due to Co(ll) is present only in thin film but absent in bulk CoHCC. Both CoHCC bulk and thin film reveals the presence of both the $Co^{II\ HS}$ and $Co^{III\ LS}$ states, thereby supporting the existence of Co^{III}-C≡N-Co^{II} link.

The intrinsic magnetic study of the CoHCC bulk and thin film was done by the X-ray magnetic circular dichroism (XMCD). The shown XMCD plot in Fig. 12b was obtained at low-temperature of 2K at an applied field of 6.8 T. As K-HCC contains cobalt in Co(lll) state, which is a diamagnetic state, no XMCD signals were observed. The intense XMCD signals occuring in both CoHCC bulk and thin film are arising due to $Co^{II\ HS}$ state. The variation in intensity between the bulk and thin film at L_3-edge ~776 eV may be due to higher composition of $Co^{II\ HS}$ in the thin film than in the bulk. The difference in the intensity

of peaks at the L_2-edge (790 eV - 795 eV region) in the CoHCC bulk and thin film is due to the different composition of spin and orbital angular magnetic moments.[19] As CoHCC thin film has more intensity in opposite sign at the L_2 edge, it is predicted to exhibit more spin magnetic moments based on the XMCD sum rules. This difference in spectra indicates different intrinsic magnetic moments and the possibility of different alignment or different composition of $Co^{II\ HS}$ spins in the CoHCC bulk and the thin film.

To get a deeper understanding of the intrinsic magnetic moments in both CoHCC bulk and thin film, a measurement is planned to study magnetization (χ-H and χ-T) plots of both the CoHCC bulk and thin film.

The color of CoHCC thin film was observed to be black and the thermochromic property which could be observed in bulk CoHCC was not evidenced in the thin film (Fig. 13) which suggests that the physical properties of material can be tuned in thin films.

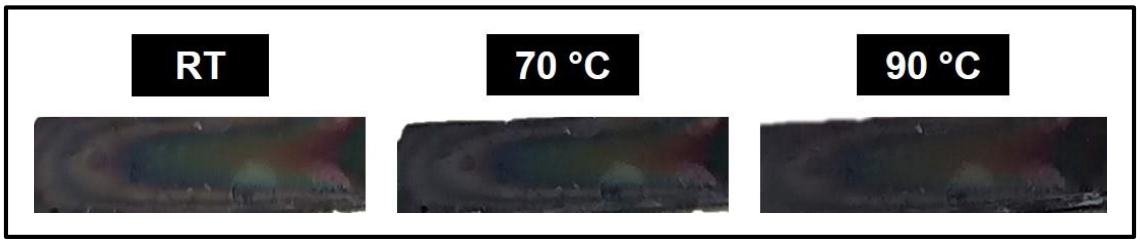

Figure 13: *Thermochromic property analyses in thin film.*

HCl Doping

FESEM revealed no change in the morphology of the thin film and the thin film remained uniform and smooth with cube-like morphology as shown in the figure. To confirm the doping of HCl, EDXS technique was employed. Homogeneous distribution of all the elements (Cl, Co, K shown in the Fig. 14b) across the thin film was observed through the elemental mapping by EDXS. The presence of chlorine was also revealed by EDXS in both the thin film (At. % = 0.63) and bulk (At. % = 0.27) CoHCC as shown in the Fig. 14(b,c). To check the stability of bulk and thin film CoHCC structure after HCl doping, we carried out the out-of-plane XRD measurements. The two peaks at ~17.5° and ~24.8°

corresponding to (200) and (220) planes indicated the intact fcc structure. But the peak ~15.1° corresponding to (111) plane which is present in thin film CoHCC becomes absent after HCl doping in thin film (Fig. 14d). The same change in the peak at ~15.1 ° in the XRD was observed upon heating the thin film at 150 °C.

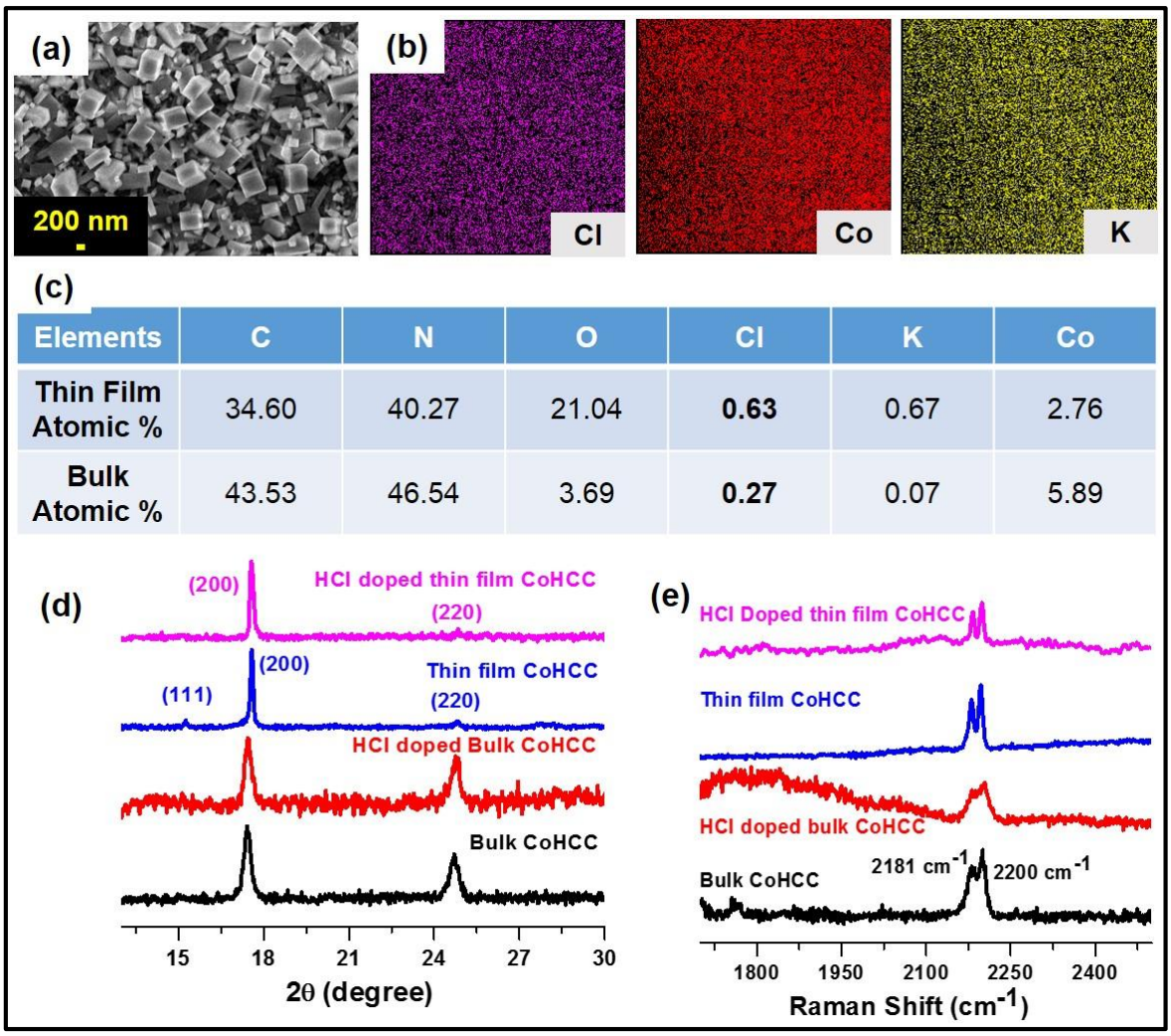

Elements	C	N	O	Cl	K	Co
Thin Film Atomic %	34.60	40.27	21.04	**0.63**	0.67	2.76
Bulk Atomic %	43.53	46.54	3.69	**0.27**	0.07	5.89

Figure 14: *(a) Zoomed-in FESEM image of HCl doped CoHCC thin film. (b) Elemental mapping of HCl doped CoHCC thin film. (c) Table showing EDXS of HCl doped CoHCC thin film and HCl doped bulk CoHCC. (d) Out of plane XRD pattern of HCl doped bulk and thin film CoHCC. (e) Raman Spectra of HCl doped bulk and thin film CoHCC.*

In Raman spectra (Fig. 14e), the cyanide stretching frequencies at ~2181 cm^{-1} and ~2200 cm^{-1} suggested the stability of mixed-valence state for Co(lll)-CN-Co(ll) even after HCl doping in both CoHCC bulk and thin film.

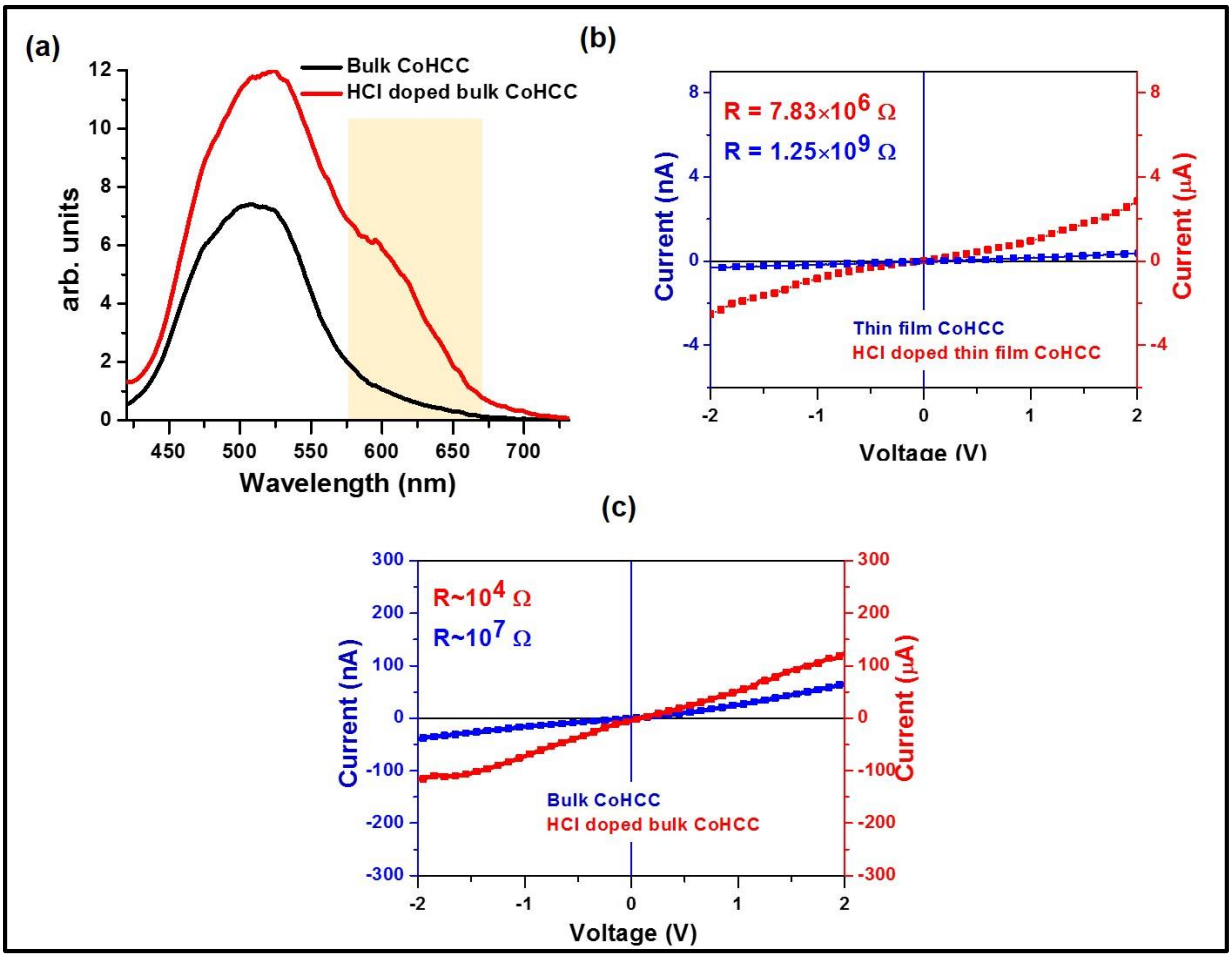

Figure 15: *(a) UV- spectra of HCl doped bulk CoHCC. (b) I-V plot of HCl doped CoHCC thin film. (c) I-V plot of HCl doped bulk CoHCC.*

In Fig. 15a, UV-vis absorption spectra of bulk CoHCC displays a strong absorption at ~515 nm which is characteristic of $^4T_1(F) \rightarrow {}^4T_1(P)$ transitions in hexacoordinated Co(ll) (O_hCo^{ll}). A distinctive absorption band at ~600 nm in the HCl doped bulk CoHCC indicates the $^4A_2(F) \rightarrow {}^4T_1(P)$ in tetracoordinated Co(ll) (T_dCo^{ll}). This transformation of O_hCo^{ll} to T_dCo^{ll} (or 6→4 coordination) was earlier recorded due to the removal of water molecules.[20] . Influence of HCl doping on bulk and thin film CoHCC was studied by two-probe I-V measurements. The CoHCC thin film and bulk were found to be insulating with the resistance of 10^9 Ω and 10^7 Ω. The resistance was immensely reduced by 2 orders and 3 orders in the thin film and bulk CoHCC respectively after HCl doping (Fig. 15c).

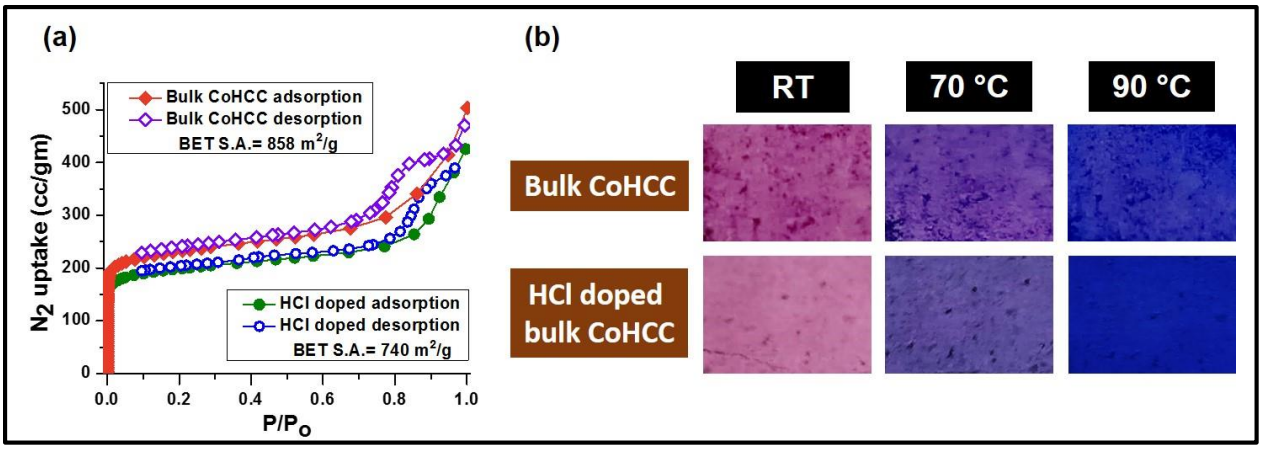

Figure 16: *(a) Nitrogen adsorption and desorption isotherms of bulk CoHCC collected at 77 K . (b) Thermochromism in bulk CoHCC before and after HCl doping.*

Effect of HCl doping on the porosity of bulk CoHCC was investigated by gas adsorption technique (Fig. 16a). Brunauer-Emmett-Teller (BET) surface area of bulk CoHCC decreased from 858 m^2/g to 740 m^2/g after HCl doping. This change in surface area is accompanied by a slight diminution in mean pore diameter from ~3.49 nm to ~3.48 nm after HCl doping in bulk CoHCC. This study reveals the retention of mesoporosity in bulk CoHCC even after HCl doping. The thermochromic property of bulk CoHCC was retained after HCl doping as shown in Fig. 16b. A change in the intensity of blue color was observed at 90 °C before and after HCl doping. At 90 °C, bulk CoHCC showed Cobalt blue color while the HCl doped bulk CoHCC exhibited royal blue color. This change also confirms the HCl doping.

6. Conclusions

First time fabrication of high-quality CoHCC thin film by robust method on both Au and Si substrates using solution deposition method involving LbL approach is reported. The thin film was found to be thermally stable by VT-PXRD. Functionalization of substrates played a crucial role for the fabrication of high-quality thin film. The thin film was analyzed to be insulating with the resistance of ~10^9 Ω. Electrical property of CoHCC thin film was modulated by HCl doping. The thermochromic feature of bulk CoHCC was not observed in the thin film configuration which suggest that physical properties of material in the thin film could be altered. Electronic structure vis-à-vis magnetic property of thin film CoHCC was realized to be significantly different from that of bulk CoHCC. It would be good to study modulation of magnetic property of CoHCC thin film by external stimuli.

7. Bibliography

[1] Hurlbutt K, Wheeler S, Capone I and Pasta M 2018 Prussian Blue Analogs as Battery Materials *Joule* **2** 1950–60

[2] Sato O, Lyoda T, Einaga Y, Fujishima A and Hashimoto K 1997 Reversible Photoinduced Magnetization *J. Electrochem. Soc.* **144** L11–3

[3] Tojo T and Engineering I 2016 Towards building next-generation batteries using a pigment electrode 1–3

[4] Verdaguer M and Girolami G S 2003 *Magnetic Prussian Blue Analogs* vol 5–5

[5] Aguilà D, Prado Y, Koumousi E S, Mathonière C and Clérac R 2016 Switchable Fe/Co Prussian blue networks and molecular analogues *Chem. Soc. Rev.* **45** 203–24

[6] Sato O, Tao J and Zhang Y Z 2007 Erratum: Control of magnetic properties through external stimuli (Angewandte Chemie - International Edition (2007) 46, (2152-2187)) *Angew. Chemie - Int. Ed.* **46** 5049

[7] Bleuzen A, Escax V, Ferrier A, Villain F, Verdaguer M, Münsch P and Itié J P 2004 Thermally induced electron transfer in a CsCoFe Prussian blue derivative: The specific role of the alkali-metal ion *Angew. Chemie - Int. Ed.* **43** 3728–31

[8] Daffé N, Jiménez J R, Studniarek M, Benchohra A, Arrio M A, Lescouëzec R and Dreiser J 2019 Direct Observation of Charge Transfer and Magnetism in Fe 4 Co 4 Cyanide-Bridged Molecular Cubes *J. Phys. Chem. Lett.* **10** 1799–804

[9] Ferlay S, Mallah T, Ouahès R, Veillet P and Verdaguer M 1995 A room-temperature organometallic magnet based on prussian blue *Nature* **378** 701–3

[10] Rana S, Prasoon A, Sadhukhan P, Jha P K, Sathe V, Barman S R and Ballav N 2018 Spontaneous Reduction of Copper(II) to Copper(I) at Solid–Liquid Interface *J. Phys. Chem. Lett.* **9** 6364–71

[11] Deng L, Yang Z, Tan L, Zeng L, Zhu Y and Guo L 2018 Investigation of the Prussian Blue Analog Co 3 [Co(CN) 6] 2 as an Anode Material for Nonaqueous

Potassium-Ion Batteries *Adv. Mater.* **30** 1–7

[12] Jiang Y, Takahashi A, Kawamoto T, Asai M, Zhang N, Lei Z, Zhang Z, Kojima K, Imoto K, Nakagawa K, Ohkoshi S I and Nakamura T 2018 High performance sorption and desorption behaviours at high working temperatures of ammonia gas in a cobalt-substituted Prussian blue analogue *Chem. Commun.* **54** 11961–4

[13] Trzciński K, Szkoda M, Szulc K, Sawczak M and Lisowska-Oleksiak A 2019 The bismuth vanadate thin layers modified by cobalt hexacyanocobaltate as visible-light active photoanodes for photoelectrochemical water oxidation *Electrochim. Acta* **295** 410–7

[14] Sam S, Chazalviel J N, Gouget-Laemmel A C, Ozanam F, Allongue P, Henry De Villeneuve C, Gabouze N and Djebbar S 2010 Covalent immobilization of amino acids on the porous silicon surface *Surf. Interface Anal.* **42** 515–8

[15] De Smet L C P M, Zuilhof H, Sudhölter E J R, Lie L H, Houlton A and Horrocks B R 2005 Mechanism of the hydrosilylation reaction of alkenes at porous silicon: Experimental and computational deuterium labeling studies *J. Phys. Chem. B* **109** 12020–31

[16] Karikalan N, Velmurugan M, Chen S M and Chelladurai K 2016 A copper hexacyanocobaltate nanocubes based dopamine sensor in the presence of ascorbic acid *RSC Adv.* **6** 48523–9

[17] McAllister W A 1970 Raman Spectrum of Potassium Hexacyanocobaltate (III) *J. Chem. Phys.* **52** 2786–7

[18] Anon 2006 *Magnetism* (Berlin, Heidelberg: Springer Berlin Heidelberg)

[19] Kuch W 2004 X-ray Magnetic Circular Dichroism for Quantitative Element-Resolved Magnetic Microscopy *Phys. Scr.* **T109** 89

[20] Zhang H, Li C, Chen D, Zhao J, Jiao X and Xia Y 2017 Facile preparation of Prussian blue analogue Co 3 [Co(CN) 6] 2 with fine-tuning color transition temperature as thermochromic material *CrystEngComm* **19** 2057–64